Effect of Combustion Chamber Configuration on In-Cylinder Air Motion of D.I. Diesel Engine

Masatoshi Shimoda, Masashi Shigemori and Shingo Tsuruoka
Hino Motors, Ltd. 3-1-1, Hinodai, Hino-shi, Tokyo

ABSTRACT

The effect of combustion chamber configuration on in-cylinder air motion of a D.I. diesel engine was investigated. The analysed combustion chambers were a flat dish type and HMMS-III (Hino micro mixing system III). The latter has 4 concaves on the periphery of the inner wall and realized better fuel consumption and lower smoke level over a wide speed range.

In this study, the oil film method was used to visualize in-cylinder air flow on the top surface of the piston near T.D.C. in the motoring condition. An axisymmetrical two dimensional laminar model for simulating the in-cylinder air motion was carried out. Further, measurement of in-cylinder air motion by L.D.V. and observation of mixture formation and burning process via high speed schlieren photography were carried out.

From these investigations on flat dish and HMMS-III combustion chambers, the contribution of HMMS-III combustion chamber to in-cylinder air motion and combustion characteristics was clarified.

INTRODUCTION

In combustion tuning of a D.I. Diesel engine, the mixture formation of the injected fuel jet and air is very important. Mixture formation mainly depends on combustion chamber configuration and distribution of fuel jet because combustion chamber configuration can control air motion within the combustion cavity (swirl and squish) and its air motion can affect distribution of the fuel jet.

The authors developed a new combustion chamber for a light duty D.I. diesel engine (HMMS-III)[1]* [2]. The combustion chamber has 4 concaves on the periphery of the cavity and realized better fuel consumption and lower smoke level than the flat dish combustion chamber over a wide speed range.

However, the effect of HMMS-III combustion chamber on in-cylinder air motion and combustion characteristics were not yet clarified.

Despite the fact that there have been many experiemental studies on in-cylinder air motion using L.D.V. and H.W.A.[3][4][5], the expression of in-cylinder air motion characteristics in the whole combustion cavity from these local measurements is very difficult.

On the otherhand, the numerical simulation method is effective for grasping in-cylinder air motion macroscopically [6][7][8], if it has been verified by experimental study as in flow visualization and L.D.V. measurement. Therefore, the combination of numerical simulation study with experimental study is effective for analysing the effect of combustion configuration on in-cylinder air motion and combustion characteristics.

In this study, in order to clarify the effects of HMMS-III combustion chamber on in-cylinder air motion and combustion characteristics, the flow visualization test using oil film method, an axisymmetrical two dimensional laminar model for simultating the in-cylinder air motion, measurement of in-cylinder air motion by L.D.V. and observation of burning process via high speed schlieren photography were carried out.

VISUALIZATION OF IN-CYLINDER AIR MOTION

In a direct injection diesel engine, the swirl and squish are the main factors of in-cylinder air motion. In has been recognized that they interfere with each other and a complex air flow is produced which has a great influence on the combustion process. Therefore, various visualization tests such as meta-aldehyde method, spark tracing method, tuft method and oil film method are effective for grasping in-cylinder air motion macroscopically.

In this study, the oil film method was used to visualize in-cylinder air flow on the top surface of piston near T.D.C. in the motiring condition. Though the pressure, temperature, air flow velocity and direction vary with the rotating angle of crankshaft in the cylinder, it was found that the streak line on the oil film easily forms at the T.D.C. in the compression stroke, and the streak line corresponds to the path line as a stationary flow[9][2].

It was thus recognized that the streak line of oil film method corresponds to the path line and in-cylinder air flow near T.D.C. can be confirmed by oil film method. A mixture of TiO_2 with oleic acid was painted thinly on the top surface

* Numbers in parentheses designate Reference at end of paper.

of the piston, and the engine was driven at constant speed. Consequently, the streak line on oil film was formed as shown in Fig. 1.

In order to clarify the direction of streak line, the oil film was spotted as shown in Fig. 2 (Spotted oil film method). Using CrPb and Pb_3O_4 instead of TiO_2, yellow and red streak lines were obtained respectively, which were suitable for classifying the complex flow field.

From Fig. 1 and 2, the streak line is recognized as shown in Fig. 3 schematically.

Namely in Fig. 3, the lines of 1 , 2 , 3 , 4 , 5 are typical streak lines. The streak line 1 was formed at the top surface of piston and mean combined vector of swirl and squish component, as shown by the dashed line in Fig. 3. The streak line 2 was formed on the valve pocket. The squich component of 2 is strong in comparison with 1 . It seems that the squish flow is pulled at the valve pocket due to difference of height between piston top surface and valve pocket. The streak line 3 was formed on the bottom surface of cavity and mean combined force of swirl and centripetal flow induced by squish flow. The centripetal flow induced by sqich flow at the bottom of vavity is presumed by numerical calculation of in-cylinder air motion as shown later.

The streak line 4 was formed at the corner of bottom surface and cavity side wall, and upward as shown in Fig. 3. A downward streak line, on the other hand, was not found. According to these streak lines, it seems that there are twin vortexes in the combustion chamber induced by squish flow as shown in Fig. 3. These twin vortexes also can be indicated by numerical calculation of in-cylinder air motion as shown later. The streak line 5 at the top of side wall seemed to be formed by a reverse-squish.

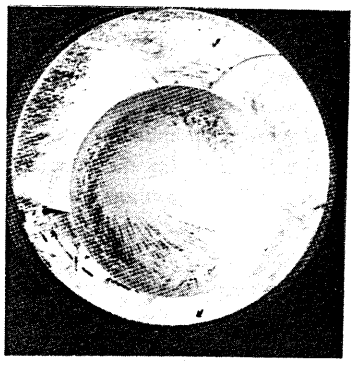

Fig. 1 - Streak lines obtained from oil film method of flat dish chamber

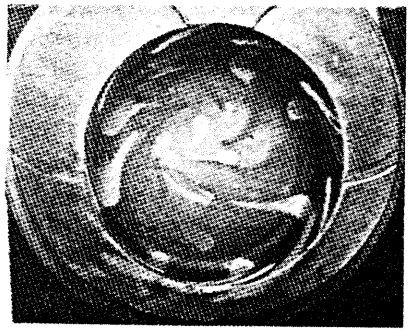

Fig. 2 - Streak lines obtained from spotted oil film method of flat dish chamber

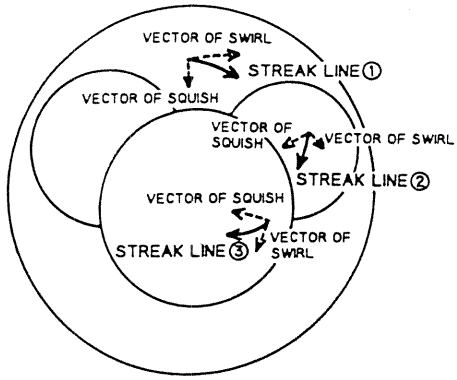

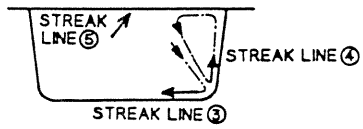

Fig. 3 - Schematical diagram of typical Streak lines

LASER DOPPLER VELOCIMETER MEASUREMENT ON A MOTORED D.I. DIESEL ENGINE

Through the oil film method is effective for grasping in-cylinder air motion macroscopically, it is not suitable for measuring change of velocity and turbulence characteristics with the rotating angle of crankshaft. In this study, in-cylinder air motion around T.D.C. of the compression stroke was measured for comparison by L.D.V.

The engine for measurement is a motored single cylinder D.I. diesel engine. The engine has a helical intake port and a quartz window, which is directly installed in the wall of the cylinder head. The seeding particles were supplied through a fluidized bed, and the exhaust air and particles were arranged to circulate via surge tank.

Fig. 4 shows the experimental optical arrangement for L.D.V. The lightsource is an Ar laser of 4 W. Method of measurement adopted was a two-beam mode back-scattering technique. The doppler signal was processed by frequency tracker. For seeding particles, soil powder (No. 11, JIS Z 8901) with a average particle size of 2 μm was employed. The particles are able to follow up the air up to a turbulent flow with maximum frequency of 5 KHz.

Fig. 5 shows a block diagram of the data processing system. The velocity signal from frequency tracker together with crank angle pulse and T.D.C. pulse, was recorded by data recorder. And the turbulence characteristics such as intensity, scale and power spectrum were processed by a fourier transform analyzer. In this study, the time-averaged method was used for determining the turbulence characteristics. The averaging interval is about 30 degrees of crank angle. The velocity signals include the holding signal, and velocity signals of 10 cycles except the signal including holding signal were averaged by the time averaged method.

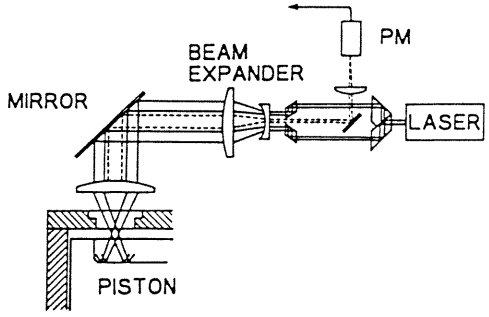

Fig. 4 - Experimental optical arrangement for L.D.V.

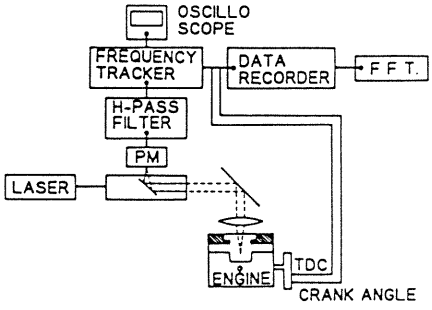

Fig. 5 - Block diagram of data processing system

Fig. 6 shows the variation in the swirl component of velocity for a point in combustion cavity. During compression stroke, the in-cylinder air is forced from outside of the piston cavity to its inside, and hence the swirl velocity increases owing to conservation of angular momentum. However, friction between the air and wall reduces the velocity. These two effects tend to cancel out during the middle part of the compression stroke. As T.D.C. is approached, the inward flow of air into the cavity becomes more significant and there is the expected rise in the swirl velocity. During the expansion stroke, though there is the expected reduction in swirl velocity.

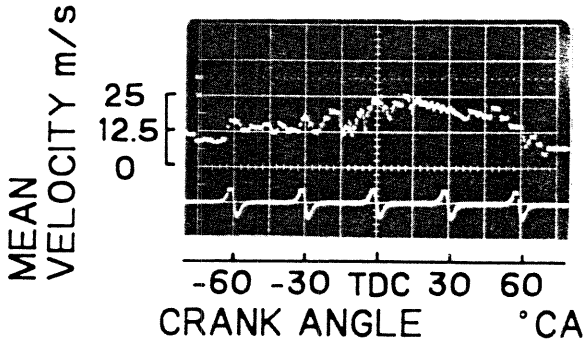

Fig. 6 - Measured swirl component of velocity for a point in combustion cavity

MATHEMATICAL MODEL FOR SIMULATING THE IN-CYLINDER AIR MOTION

An axisymmetrical two dimensional model in respect to the cylinder aixs was conceived, and the density and viscosity of the in-cylinder air were assumed to spacially uniform. Novier – Stokes equations and the equation of continuity in co-ordinate system (r, θ, z) were expressed as follows:

$$\frac{\partial Vr}{\partial t} + Vr\frac{\partial Vr}{\partial r} - \frac{V\theta^2}{r} + Vz\frac{\partial Vr}{\partial z} = -\frac{1}{\rho}\frac{\partial P}{\partial r} + \nu\left(\frac{\partial^2 Vr}{\partial r^2} + \frac{1}{r}\frac{\partial Vr}{\partial r} - \frac{Vr}{r^2} + \frac{\partial^2 Vr}{\partial z^2}\right)$$

$$\frac{\partial Vz}{\partial t} + Vr\frac{\partial Vz}{\partial r} + Vz\frac{\partial Vz}{\partial z} = -\frac{1}{\rho}\frac{\partial P}{\partial z} + \nu\left(\frac{\partial^2 Vz}{\partial r^2} + \frac{1}{r}\frac{\partial Vz}{\partial r} + \frac{\partial^2 Vz}{\partial z^2}\right)$$

$$\frac{\partial V\theta}{\partial t} + Vr\frac{\partial V\theta}{\partial r} + \frac{VrV\theta}{r} + Vz\frac{\partial V\theta}{\partial z} = \nu\left(\frac{\partial^2 V\theta}{\partial r^2} + \frac{1}{r}\frac{\partial V\theta}{\partial r} - \frac{V\theta}{r^2} + \frac{\partial^2 V\theta}{\partial z^2}\right)$$

$$\frac{\partial Vr}{\partial r} + \frac{Vr}{r} + \frac{\partial Vz}{\partial z} = \frac{1}{B}\frac{\partial B}{\partial t}$$

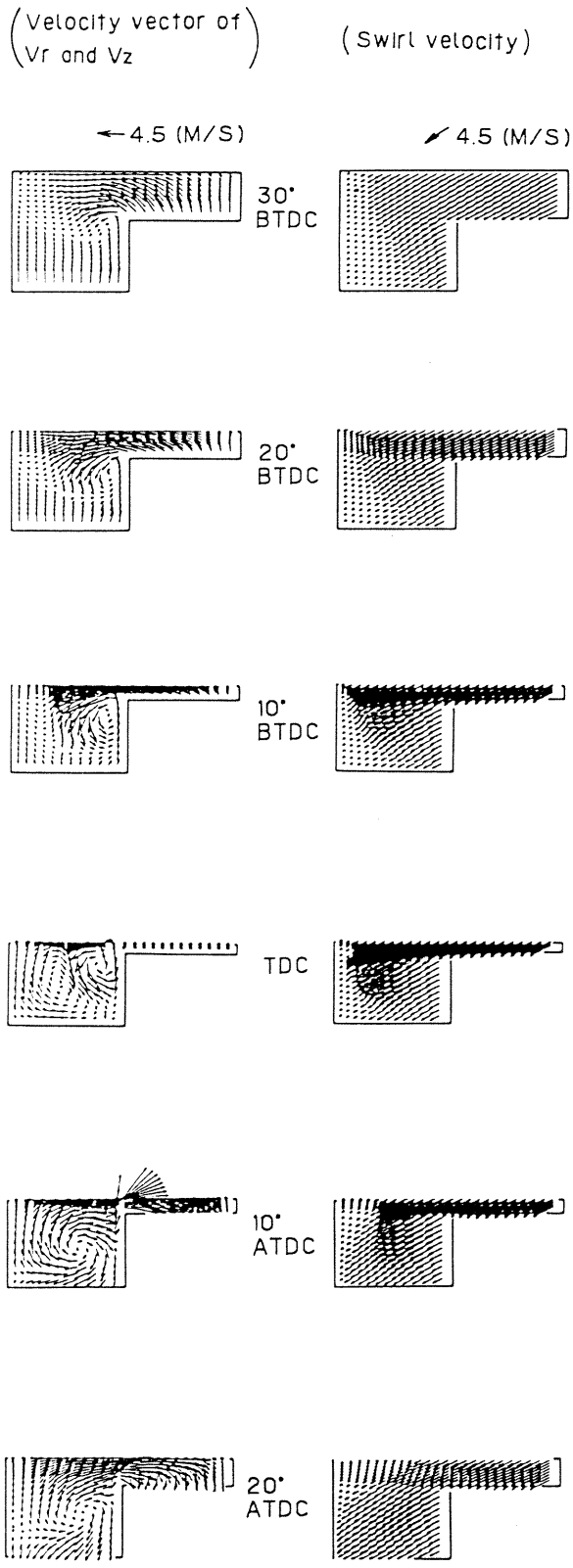

Fig. 7 - Calculated velocity field in axial-radial plane

Vr : velocity of radial component
Vz : velocity of axial component
Vθ : velocity of swirl component
P : pressure
ρ : density
B : volume of combustion chamber

The above equations were transformed into the finite-difference form. The computer code is this study is the same one as Matsuoka and Kamimoto's[10]. The calculation conditions are as follows:

molecular viscosity as kinetic viscosity
free slip boundary condition at the wall
an engine speed of 1,000 rpm
swirl ratio of 1.0

Fig. 7 shows calculated result in flat dish combustion chamber. At the bottom in Fig. 7 is swirl velocity distribution and at the top is velocity vectrol distribution in axial cross section. In this figure at T.D.C., the centripetal flow induced squish flow at the bottom of cavity and twin vortexes as expected by the oil film method are recognized. An increase of swirl velocity in combustion cavity as measured by L.D.V. is also recognized. Therefore, man recognized that this mathematical model can simulate actual in-cylinder air motion in combustion cavity near T.D.C.

EFFECT OF COMBUSTION CHAMBER CONFIGURATION

Engine Performance

Fig. 8 shows a comparison of combustion chamber configurations between flat dish and HMMS-III. HMMS-III combustion chamber has 4 concaves on the periphery of cavity and realized better fuel consumption and lower smoke level than the flat dish combustion chamber over a wide speed range as shown in Fig. 9.

Fig. 10 shows a comparison of combustion characteristics between both combustion cavities. The HMMS-III has a distinctive effect of shortening the combustion period by shorter ignition delay and active reaction in the second stage of combustion region.

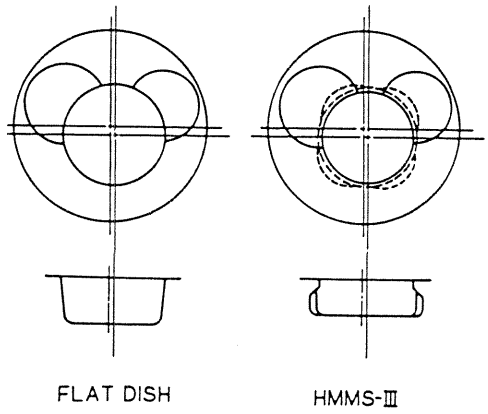

Fig. 8 - Comparison of combustion chamber configurations

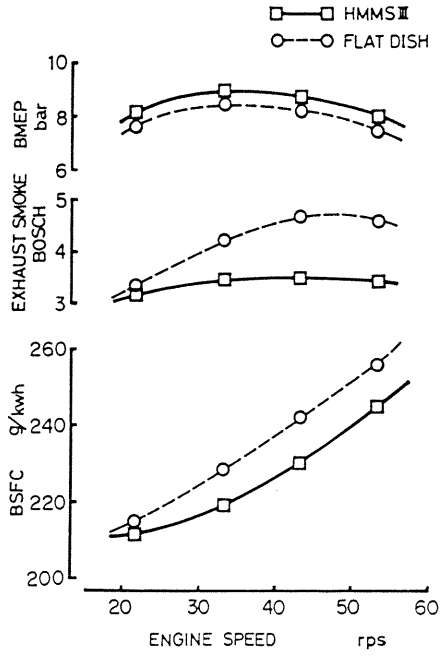

Fig. 9 - Comparison of engine performance of HMMS-Ⅲ and flat dish

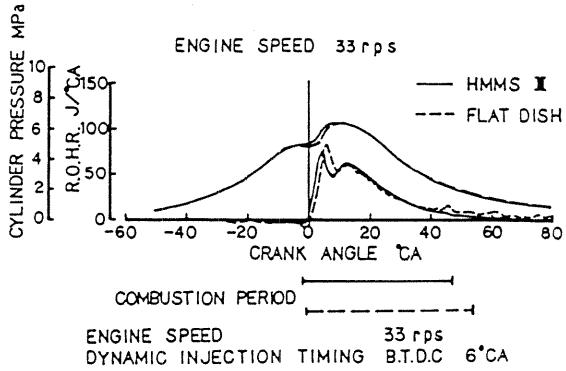

Fig. 10 - Comparison of rate of heat release curves of flat dish chamber and HMMS-Ⅲ

Visualization of In-Cylinder Air Motion

The streak lines of both combustion chambers by oil film method and spotted oil film method are shown in Fig.11.

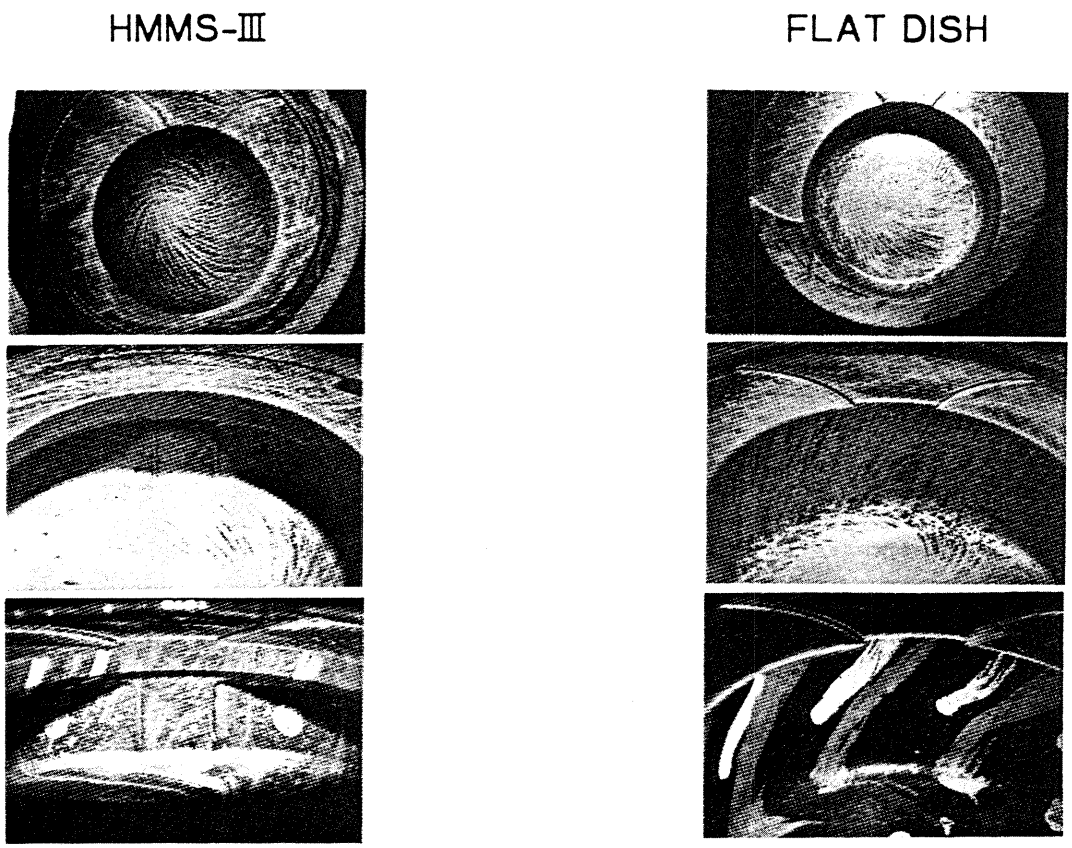

Fig. 11 - Comparison of streak lines of obtained from oil film method and spotted oil film method

Upon comparing streak lines of the combustion chambers, the center of the air swirl is located at almost the center of the combustion cavity for the HMMS-III, while at the flat dish it is offset. For the HMMS-III, many fine and upward streak lines are found in the 4 concaves. It seems to prove that the vortex induced by squish invades the 4 concaves of HMMS-III and grows as is schematically shown in Fig.12. And also the 4 vortexes which invade the 4 concaves of HMMS-III can erupt from the concaves to the cavity when the swirl declines in the expansion stroke.

Such a flow can give the swirling air in the cavity a centripetal force and will cause the swirl to be located almost at the center of the combustion cavity for the HMMS-III. Moreover, it can be considered that such a flow promotes a better mixing at the diffusion burning period and contributes to reduction of fuel consumption and exhaust smoke.

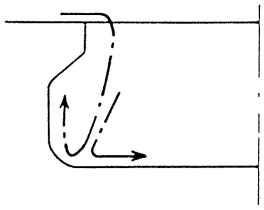

Fig. 12 - Schematical diagram of the vortex of HMMS-III

Laser Doppler Velocimeter Measurement

Fig. 13 shows mean velocity, turbulence intensity and the integral spatial scale of these combustion chamber configurations. From this figure, turbulence intensity of HMMS-III is larger and its integral spatial scale is smaller during crank angle from T.D.C. to 30° A.T.D.C. The turbulent power spectrums of these combustion chamber configurations during crank angle from T.D.C. to 30° A.T.D.C. are shown in Fig.14. It is found from this figure that the HMMS-III has a higher distribution of higher frequency range while the flat dish has comparatively low distribution of the same frequencies.

The turbulence characteristics of HMMS-III are concluded as follows;

(1) the turbulence intensity is large
(2) the integral spatial scale is small
(3) the turbulent power spectrum has a higher distribution of higher frequency range

It can be considered that these turbulence characteristics correspond with the eruption from concave to cavity observed by the oil film method. The activity of swirl motion owing to the eruption during crank angle from T.D.C. to 30° A.T.D.C. seems to contribute to better mixing of fuel jet and air, and gives active reaction in the diffusion burning period, and also induces reduction of fuel consumption and exhaust smoke level.

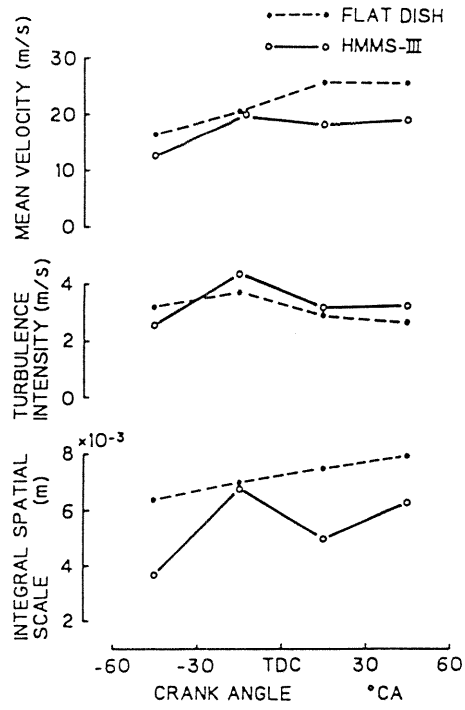

Fig. 13 - Comparison of the turbulence characteristics in each combustion cavity configuration

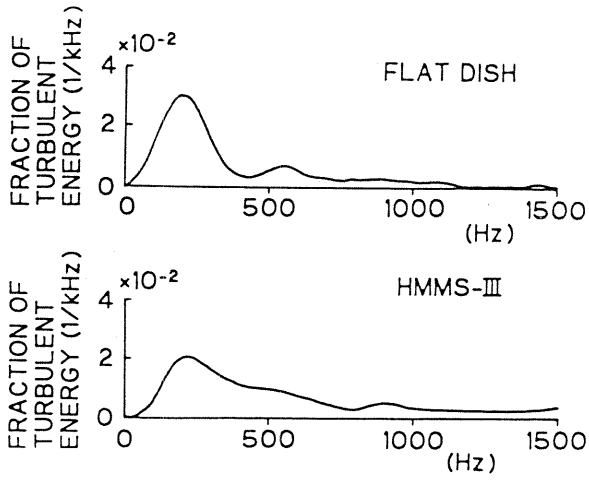

Fig. 14 - Comparison of the turbulent power spectrums in each combustion cavity configuration

Mathematical Model for Simulating the In-Cylinder Air Motion

Fig. 15 shows a comparison of calculated results between flat dish and HMMS-III. In the case of HMMS-III, the vortex induced by squish invades the 4 concaves and grows. This calculated result corresponds to the result of flow visualization test. Comparing swirl velocity distribution at 20° A.T.D.C. between both combustion chambers, the swirl velocity of HMMS-III at cavity bottom and middle between cylinder center and cavity wall is larger than that of the flat dish. This calculation result corresponds to eruption of 4 vortexes to the cavity as expected by flow visualization and L.D.V. measurement.

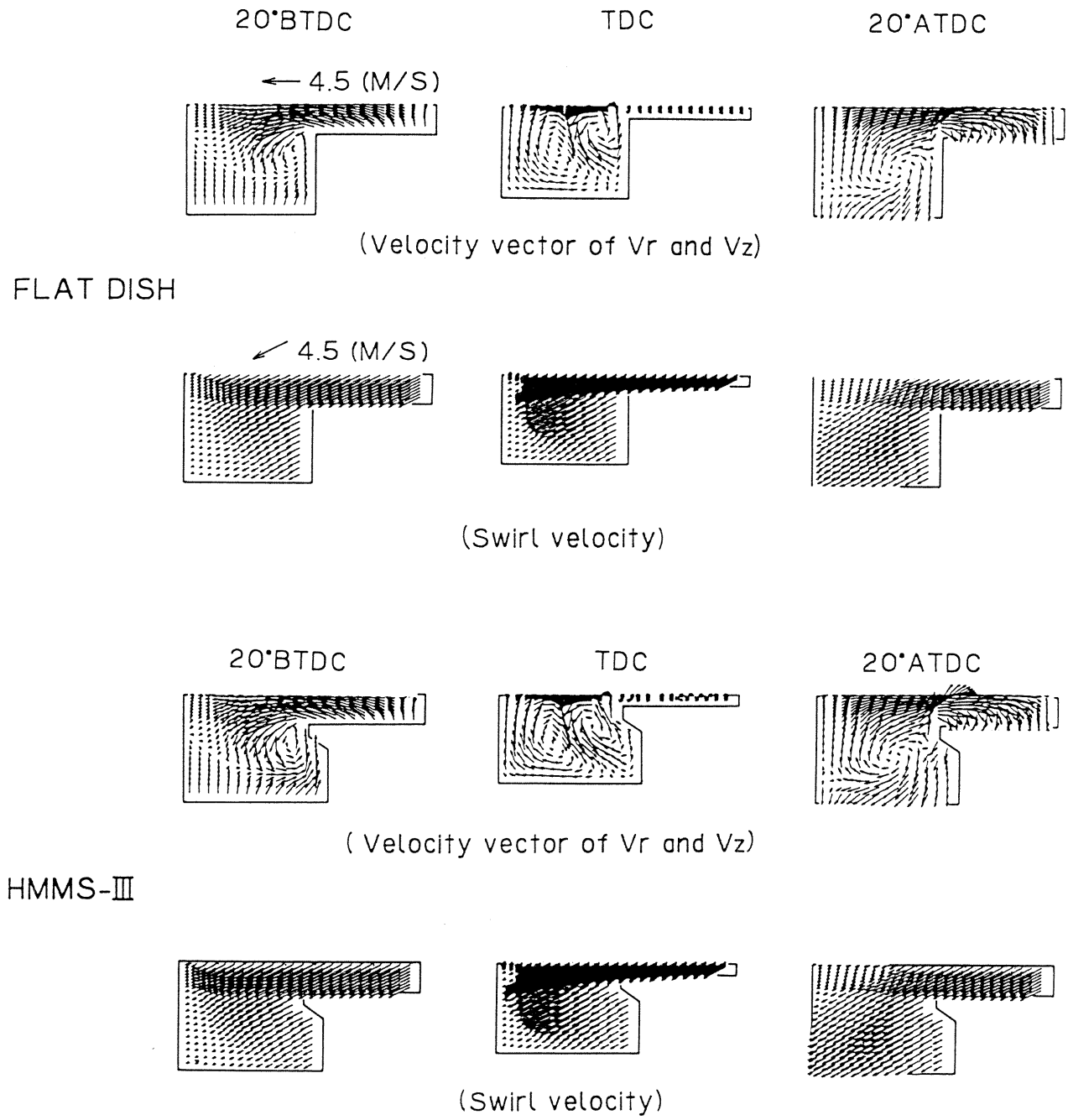

Fig. 15 - Comparison of calculated velocity field in axial-radial plane

OBSERVATION OF COMBUSTION PROCESS OF HMMS-III VIA HIGH SPEED SCHLIEREN PHOTOGRAPHY

As mentioned before, there is a phenomenon of eruption from concave to cavity at HMMS-III as expexted from both analysis by the oil film method and L.D.V. The high speed schlieren photography was carried out both on motoring and firing condition to confirm the eruption. Fig. 16 shows the experimental optical arrangement for schlieren photography at the test engine. Fig. 17 shows photographs of certain selected frames of the air motion in motoring condition of HMMS-III. It is found that a peculiar air movement erupts from concave to cavity of HMMS-III, and these peculiar air movement corresponds to the phenomena expected by the oil film method and L.D.V. Fig. 18 shows also photographs of certain selected frames of the combustion sequence on HMMS-III. At 14.6° and 15.8° A.T.D.C. in this figure, the flame also erupts from the concaves of the combustion cavity. It seems that the peculiar movement of the flame, which depends on configuration of HMMS-III, promotes a strong mixing at the diffusion burning region and contributes to reduction of combustion period which induces good fuel consumption and less exhaust smoke.

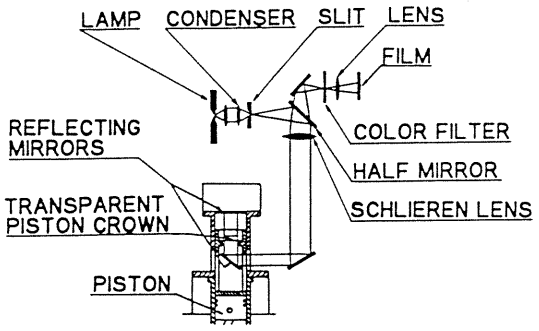

Fig. 16 - Experimental optical arrangement for schlieren photography

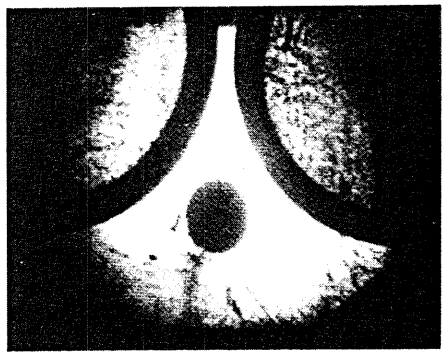

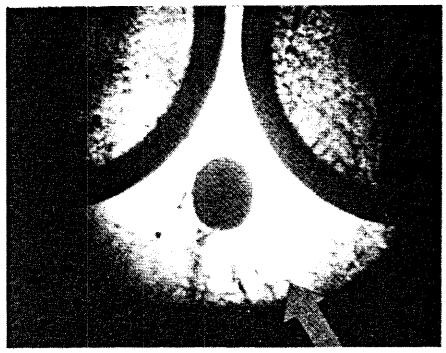

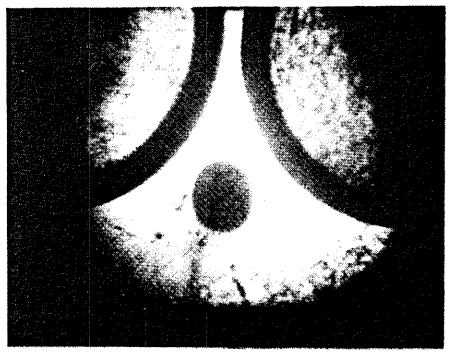

Fig. 17 - Schlieren photographs of certain selected frames of air motion in motoring condition

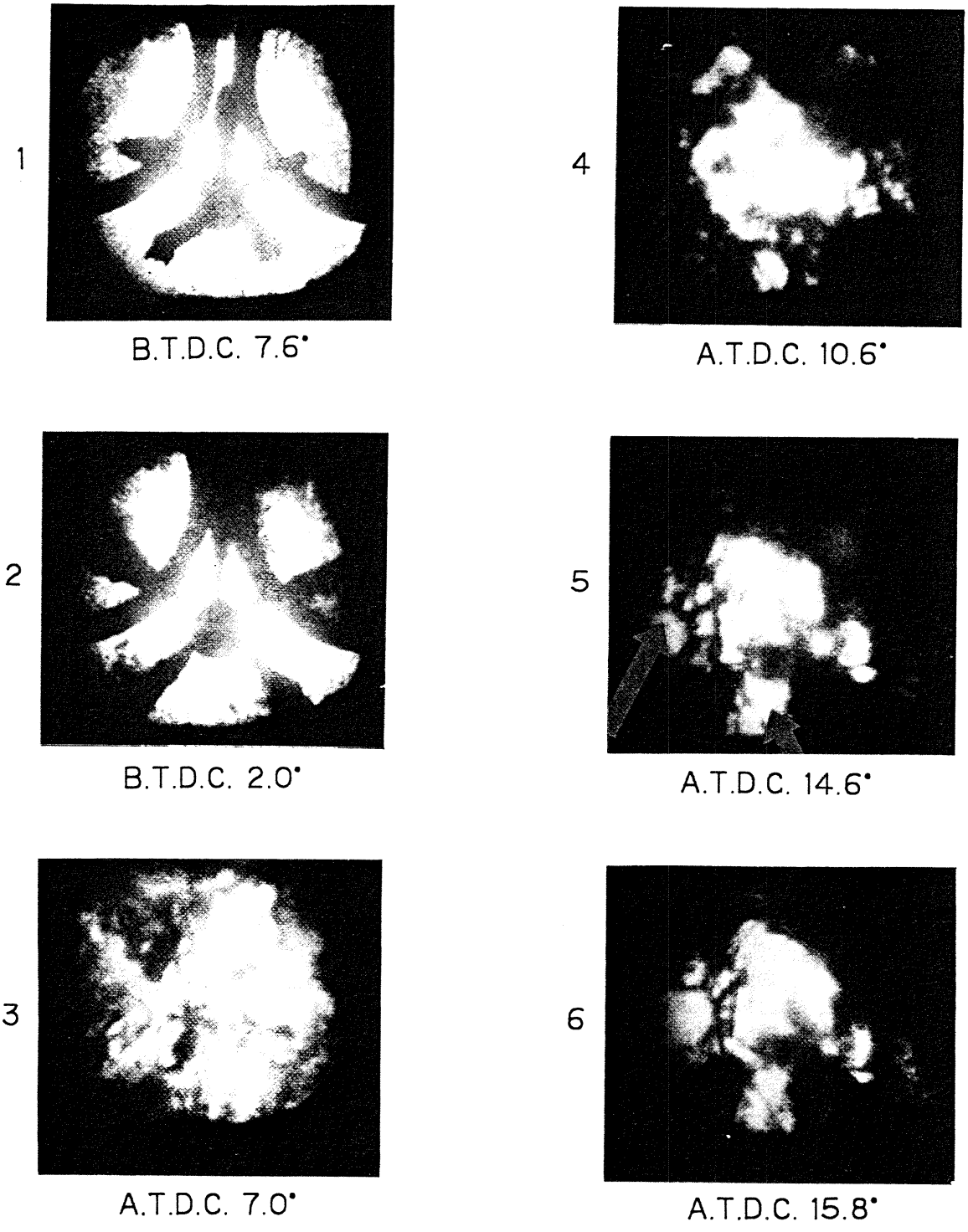

Fig. 18 - Schlieren photographs of certain selected frames of the combustion sequence on HMMS-III

CONCLUSION

The effect of HMMS-III combustion chamber configuration on in-cylinder air motion and combustion characteristics was investigated. The main conclusions are as follows;

1. It was recognized from flow visualization test and mathematical calculation in the case of HMMS-III that the vortex induced by squish invades the 4 concaves and grows.
2. The four vortexes which invade the 4 concaves of HMMS-III can erupt from concave to cavity when the swirl declines in the expansion stroke.
3. This eruption occurs in firing condition as recognized by high speed schlieren photography. It promotes a strong mixing at the diffusion burning region and contributes to reduction of combustion period which induces good fuel consumption and less exhaust smoke.

ACKNOWLEDGMENT

The authors wish thank Professor Emeritus S. Matsuoka and Associate Professor T. Kamimoto of Tokyo Institute of Technology for their generous advice in the studies mentioned herein. The authors are also thankful to the directors of Hino Motors, Ltd. for their permission to publish paper.

REFERENCE

1. M. Shigenori, et al., "Development of Combustion System for a Light Duty D.I. Diesel Engine", SAE 831296, 1983
2. M. Shimoda, et al., "Effect of Combustion Chamber Configuration on In-Cylinder Air Motion and Combustion Characteristics of D.I. Diesel Engine" SAE 850070, 1985
3. C.N.F. Waterhouse, et al., "High Speed Data Logging from the LDV", DP82/1503 RICARDO Consulting Engineers, 1982
4. P.O. Witze, "A Critical Comparison of Hot-Wire Anemometry and Laser Doppler Velocimetry for I.C. Engine Application". SAE 800132, 1980
5. T.J. Williams, et al., "Gas Flow Studies in Direct Injection Diesel Engine with Re-Entrant Combustion Chamber", SAE 800027, 1980
6. A.D. Gosman, et cl., "Calculation of Three Dimentional Air Motion in Model Engine", SAE 840229, 1984
7. V.K. Duggal, et al., "Three-Dimensional Modeling of In-Cylinder Processes in D.I. Diesel Engine", SAE 840227, 1984
8. S.H. El Tahry, et al., "A Nemerical Study on the Effects of Fluid Motion at Inlet-Valve Closure on Subsequent Fluid Motion in a Motord Engine", SAE 820035 1982
9. Y. Hamamoto, et al., "Visualization of Boundary Layer Flow on Piston Crown of Internal Combustion Engine", Four Symposium on Flow Visualization, Institute of Space and Aeronautical Science, University of Tokyo, 1976, (Japanese)
10. S. Matsuoka, et al., "LDA Measurement and a Theoretical Analysis of the In-Cylinder Air Motion in a D.I. Diesel Engine" SAE 850106, 1985